PHENIX Measurements of dNch/dη in small systems

Available online at www.sciencedirect.com

ScienceDirect

Nuclear Physics A 982 (2019) 839–842

NUCLEAR PHYSICS A

www.elsevier.com/locate/nuclphysa

XXVIIth International Conference on Ultrarelativistic Nucleus-Nucleus Collisions (Quark Matter 2018)

PHENIX Measurements of $dN_{ch}/d\eta$ in small systems

D. McGlinchey (for the PHENIX collaboration)

Los Alamos National Laboratory, Los Alamos, NM 87545

Abstract

The PHENIX experiment has excellent data for small systems including p+Au, d+Au, ^{3}He+Au at 200 GeV as well as the d+Au beam energy scan down to 19.6 GeV. We present new measurements of $dN_{ch}/d\eta$ for all of these systems over a broad range in pseudorapidity $-3 < \eta < +3$ and event multiplicity. These measurements provide key constraints of baryon stopping models and are compared with various theoretical calculations. The measurements are also compared with flow observables as a function of pseudorapidity to explore scaling relations. In particular measurements as a function of collision energy provide key inputs for calculations for the upcoming A+A beam energy scan at RHIC in terms of particle production and baryon rapidity shifts.

1. Introduction

Measurements of the longitudinal dependence of particle production in highly asymmetric collision systems can provide important insights into particle production mechanisms which can not be gained from larger, symmetric collision systems alone. From 2014–2016, the PHENIX experiment at RHIC has collected excellent data sets for "small system" which include p+Al, p+Au, d+Au, and ^{3}He+Au collisions at $\sqrt{s_{NN}}$ = 200 GeV, as well as d+Au collisions at $\sqrt{s_{NN}}$ = 19.6, 39, and 62.4 GeV. Measurements of charged particle yield, $dN_{ch}/d\eta$, as a function pseudorapidity, η, in all these systems can provide stringent constraints on particle production models.

Detailed understanding of the production mechanisms is important in its own right, but additionally provides the initial energy density profile required as an input for 3D hydrodynamic models. Constraining these initial conditions provide an additional piece of the puzzle in our understanding of the origin of the observed azimuthal anisotropies in these small collision systems (See Ref. [1] for a recent review).

2. Particle production in the d+Au beam energy scan

In 2016, RHIC performed an energy scan of d+Au collisions, with energies of $\sqrt{s_{NN}}$ = 200, 62.4, 39, and 19.6 GeV with the goal of understanding the energy dependence of the measured azimuthal anisotropies

https://doi.org/10.1016/j.nuclphysa.2018.08.030

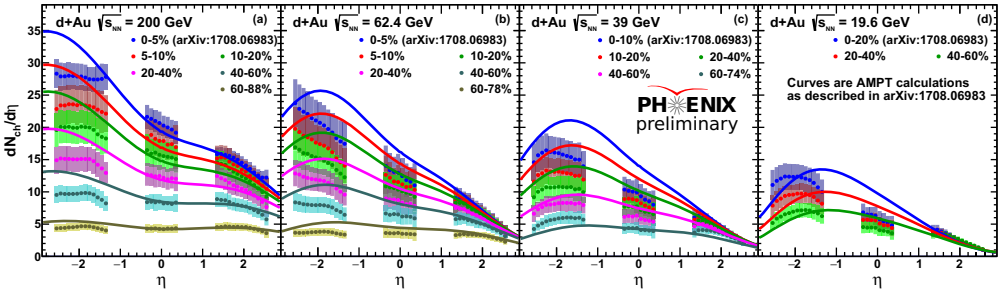

Fig. 1. The $dN_{ch}/d\eta$ as a function of η and event centrality in d+Au collisions at ($\sqrt{s_{NN}}$ = 200 (a), 62.4 (b), 39 (c), and 19.6 (d) GeV. The curves are calculations from AMPT [5].

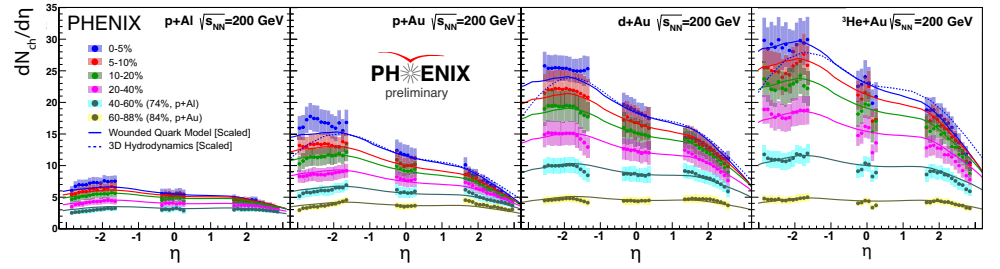

Fig. 2. The $dN_{ch}/d\eta$ as a function of η and event centrality in (from left to right) p+Al, p+Au, d+Au, and ^{3}He+Au collisions at $\sqrt{s_{NN}}$ = 200 GeV. The solid curves are predictions from a wounded quark emission function model [6]. The dashed curves are predictions for 0-5% central events from 3D hydrodynamics [7].

in small systems and their link to a hydrodynamic description. The measurement of $dN_{ch}/d\eta$ as a function of η in central collisions at all four energies was detailed in Ref. [2]. In order to minimize the uncertainties inherent in an absolute normalization correction, the analyses used a "bootstrapping" method, where the raw yield in 0-20% central d+Au collisions at $\sqrt{s_{NN}}$ = 200 GeV was normalized to previous measurements by the PHOBOS collaboration [3]. This same normalization was applied to measurements of the yield ratios between the collision energies. The results were in excellent agreement with previous PHENIX measurements at midpsuedorapidity [4]. This same analysis procedure was then extended to cover the full centrality range, the preliminary results of which are shown in Fig. 1.

In Fig. 1, the measurements are compared with calculations from AMPT [5], where centrality is determined following a similar procedure. Starting with the results at 200 GeV, AMPT provides a reasonable description of the $dN_{ch}/d\eta$ at mid and forward (d-going) pseudorapidities, while overestimating the results at backward (Au-going) pseudorapidities. This may be caused by the centrality, defined in the region $-3.9 < \eta < -3.1$, causing an auto-correlation bias in the neighboring regions than is seen in the data. This general trend is seen at the lower collision energies, with the addition that AMPT consistently overestimates the $dN_{ch}/d\eta$ even at midpseudorapitidy

3. Particle production in the geometry scan

Using the same analysis methodology described above, preliminary measurements of the pseudorapidity dependence of $dN_{ch}/d\eta$ have now been made across all the small collision species run at RHIC. This includes p+Al, p+Au, d+Au, and ^{3}He+Au at $\sqrt{s_{NN}}$ = 200 GeV from data collected between 2014 and 2016. The results are shown as a function of η, binned in centrality, in Fig. 2. The effects of moving from the smallest

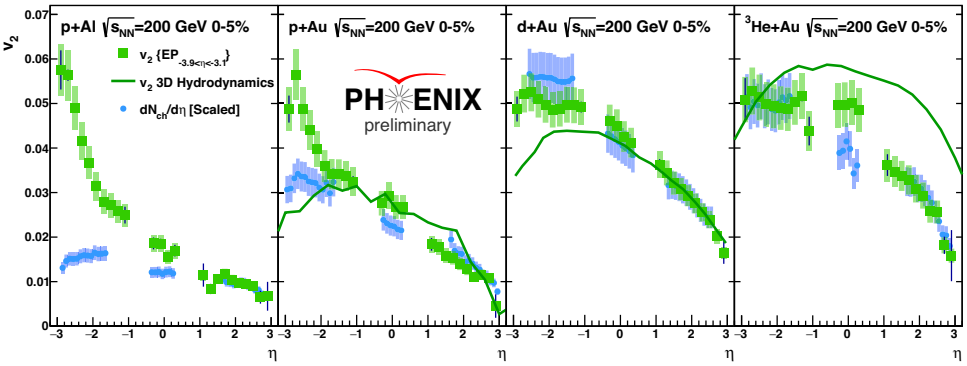

Fig. 3. Measured v_2 as a function of η (closed green squares) compared to scaled $dN_{ch}/d\eta$ (closed blue circles) in 0-5% central (from left to right) p+Al, p+Au, d+Au, and ^{3}He+Au collisions at $\sqrt{s_{NN}}$ = 200 GeV. The solid green curves are predictions from hydrodynamics [8].

(p+Al) to the largest (^{3}He+Au) collision systems can be clearly seen in the $dN_{ch}/d\eta$ increase at central pseudorapidity by a factor of five.

These data can provide important constraints on particle production models. Predictions from one such model which utilizes wounded quark emission functions [6] are compared to the data in Fig. 2. In this model, pseudorapidity dependent wounded quark emission functions are extracted from fits to previously published $dN_{ch}/d\eta$ results from the PHOBOS collaboration [3]. The universality of these emission functions are tested by predicting the centrality and η dependence of $dN_{ch}/d\eta$ across the small collision systems. As the η dependence of the predictions carry most of the information, the calculations have been normalized to the data. The predictions are in good agreement with the data across all centralities and collision systems.

Also shown in Fig. 2 are predictions from a 3D hydrodynamic model [7] for 0-5% central p+Au, d+Au, and ^{3}He+Au at $\sqrt{s_{NN}}$ = 200 GeV. As was done for the wounded quark emission model, the calculations are scaled to the data, as the shape of the distribution is more important than the normalization. In all three systems, the shape of the distribution describes the data well at mid and forward pseudorapidities. However, the $dN_{ch}/d\eta$ appears to fall off faster at backward pseudorapidity than is seen in the data.

4. Pseudorapidity dependence of elliptic flow

It was observed in 0-5% central d+Au collisions at $\sqrt{s_{NN}}$ = 200 and 62.4 GeV, that measurements of the p_T integrated v_2 as a function of η appear to scale with the measured $dN_{ch}/d\eta$ [2]. This has now been further tested with measurements of $v_2(\eta)$ in 0-5% central p+Al, p+Au, and ^{3}He+Au collisions at $\sqrt{s_{NN}}$ = 200 GeV, as shown in Fig. 3. As was done in the d+Au case, the $dN_{ch}/d\eta$ has been scaled down and compared with the shape of the $v_2(\eta)$. Focusing on the mid and forward pseudorapidity regions, the general shape is similar between $dN_{ch}/d\eta$ and $v_2(\eta)$, however there does not appear to be an exact scaling, as implied by the d+Au alone. At backward pseudorapidity, there appears to be a striking departure from this qualitative scaling, with the $v_2(\eta)$ increasing drastically at backward pseudorapidity. This is likely due to nonflow effects, as the v_2 is measured using the event plane method where the event plane is determined in the region $-3.9 < \eta < -3.1$. Moving towards backward rapidity reduces the $\Delta\eta$ gap, which is known to increase the nonflow contribution, particularly in these small collision systems.

Also shown in Fig. 3 are predictions from hydrodynamics [8]. In p+Au and d+Au collisions, the hydro calculations describe the mid and forward pseudorapidity distribution well, however they appear to drop faster at backward pseudorapidity than seen in the data, with the caveat that the backward pseudorapidity region is the most susceptible to nonflow contributions. The results in ^{3}He+Au significantly overestimate the data, which may be due to an overestimate of the $dN_{ch}/d\eta$ in the ^{3}He+Au compared to d+Au and p+Au.

5. Summary

PHENIX has presented new preliminary results on a comprehensive analysis of charged particle multiplicity in small collision systems with measurements of $dN_{ch}/d\eta$ vs η in bins of event centrality for p+Al, p+Au, d+Au, and ^{3}He+Au collisions at $\sqrt{s_{NN}}$ = 200 GeV as well as d+Au collisions at $\sqrt{s_{NN}}$ = 19.6, 39, and 62.4 GeV. These results can provide strong constraints on the longitudinal dependence of particle production models. Predictions from a wounded quark model provide good descriptions of the shape of the $dN_{ch}/d\eta$ distribution across η, centrality, and collision system at $\sqrt{s_{NN}}$ = 200 GeV. Predictions from a 3D hydrodynamic model also provide good descriptions of the shape at mid and forward pseudorapidities, but appear to drop faster at backward pseudorapidity than is observed in the data.

Additionally, PHENIX has measured the p_T integrated $v_2(\eta)$ using the event plane method in 0-5% central p+Al, p+Au, d+Au, and ^{3}He+Au collisions at $\sqrt{s_{NN}}$ = 200 GeV. Hydrodynamic calculations agree with the data at mid and foward pseudorapidity in p+Au and d+Au collisions, however overpredict the measurements in ^{3}He+Au. In all cases, the calculations fall off at backward pseudorapidity faster than seen in the data. The scaling of $v_2(\eta)$ with $dN_{ch}/d\eta$ observed in d+Au collisions does not appear to hold in the other systems.

References

[1] J. L. Nagle, W. A. Zajc, Small System Collectivity in Relativistic Hadron and Nuclear CollisionsarXiv:1801.03477.
[2] C. Aidala, et al., Measurements of azimuthal anisotropy and charged-particle multiplicity in d+Au collisions at $\sqrt{s_{NN}}$ =200, 62.4, 39, and 19.6 GeV, Phys. Rev. C96 (6) (2017) 064905. doi:10.1103/PhysRevC.96.064905.
[3] B. B. Back, et al., Scaling of charged particle production in d + Au collisions at $\sqrt{s_{NN}}$ = 200-GeV, Phys. Rev. C72 (2005) 031901. doi:10.1103/PhysRevC.72.031901.
[4] A. Adare, et al., Transverse energy production and charged-particle multiplicity at midrapidity in various systems from $\sqrt{s_{NN}}$ = 7.7 to 200 GeV, Phys. Rev. C93 (2) (2016) 024901. doi:10.1103/PhysRevC.93.024901.
[5] Z.-W. Lin, C. M. Ko, B.-A. Li, B. Zhang, S. Pal, A Multi-phase transport model for relativistic heavy ion collisions, Phys. Rev. C 72 (2005) 064901. doi:10.1103/PhysRevC.72.064901.
[6] M. Barej, A. Bzdak, P. Gutowski, Wounded-quark emission function at the top energy available at the BNL Relativistic Heavy Ion Collider, Phys. Rev. C97 (3) (2018) 034901. doi:10.1103/PhysRevC.97.034901.
[7] P. BoÅek, W. Broniowski, Collective flow in ultrarelativistic 3HeAu collisions, Physics Letters B 739 (2014) 308 – 312. doi:https://doi.org/10.1016/j.physletb.2014.11.006.
[8] P. Bozek, W. Broniowski, Collective flow in ultrarelativistic ^{3}He-Au collisions, Phys. Lett. B 739 (2014) 308. doi:10.1016/j.physletb.2014.11.006.